RESEARCH ARTICLE

Metabolite Signature of Alzheimer's Disease in Adults with Down Syndrome

Victor Montal,[1,2] Isabel Barroeta,[1,2] Alexandre Bejanin,[1,2] Jordi Pegueroles,[1,2] María Carmona-Iragui,[1,2,3] Miren Altuna,[1,3] Bessy Benejam,[3] Laura Videla,[1,3] Susana Fernández,[3] Concepcion Padilla,[1] Mateus Aranha,[1] Florencia Iulita,[1,2] Didac Vidal-Piñeiro,[4] Daniel Alcolea,[1,2] Rafael Blesa,[1,2] Alberto Lleó,[1,2] and Juan Fortea,[1,2,3] Down Alzheimer Barcelona Neuroimaging Initiative

Objective: The purpose of this study was to examine the Alzheimer's disease metabolite signature through magnetic resonance spectroscopy in adults with Down syndrome and its relation with Alzheimer's disease biomarkers and cortical thickness.

Methods: We included 118 adults with Down syndrome from the Down Alzheimer Barcelona Imaging Initiative and 71 euploid healthy controls from the Sant Pau Initiative on Neurodegeneration cohort. We measured the levels of myo-inositol (a marker of neuroinflammation) and N-acetyl-aspartate (a marker of neuronal integrity) in the precuneus using magnetic resonance spectroscopy. We investigated the changes with age and along the disease continuum (asymptomatic, prodromal Alzheimer's disease, and Alzheimer's disease dementia stages). We assessed the relationship between these metabolites and $A\beta_{42}/A\beta_{40}$ ratio, phosphorylated tau-181, neurofilament light (NfL), and YKL-40 cerebrospinal fluid levels as well as amyloid positron emission tomography uptake using Spearman correlations controlling for multiple comparisons. Finally, we computed the relationship between cortical thickness and metabolite levels using Freesurfer.

Results: Asymptomatic adults with Down syndrome had a 27.5% increase in the levels of myo-inositol, but equal levels of N-acetyl-aspartate compared to euploid healthy controls. With disease progression, myo-inositol levels increased, whereas N-acetyl-aspartate levels decreased in symptomatic stages of the disease. Myo-inositol was associated with amyloid, tau, and neurodegeneration markers, mainly at symptomatic stages of the disease, whereas N-acetyl-aspartate was related to neurodegeneration biomarkers in symptomatic stages. Both metabolites were significantly associated with cortical thinning, mainly in symptomatic participants.

Interpretation: Magnetic resonance spectroscopy detects Alzheimer's disease related inflammation and neurodegeneration, and could be a good noninvasive disease-stage biomarker in Down syndrome.

ANN NEUROL 2021;00:1–10

The lifetime risk of symptomatic Alzheimer's disease (AD) in adults with Down syndrome (DS) is over 90%.[1] This ultra-high risk is mainly caused by the extra copy of the amyloid precursor protein gene, coded on chromosome 21. DS is consequently conceptualized as a genetically determined form of AD.[2] The clinical and biomarker changes of AD in adults with DS are strikingly similar to those described in autosomal dominant AD (ADAD).[3] DS thus offers, likewise ADAD, a unique opportunity to determine the sequence of changes from preclinical AD to symptomatic stages.[3]

The study of regional metabolite levels using proton magnetic resonance spectroscopy (MRS) has shown potential to track brain alterations in vivo along the AD

View this article online at wileyonlinelibrary.com. DOI: 10.1002/ana.26178

Received Jan 18, 2021, and in revised form Jul 21, 2021. Accepted for publication Jul 23, 2021.

Address correspondence to Dr Juan Fortea, Memory Unit, Department of Neurology, Hospital de Sant Pau C\Sant Antoni Maria Claret, 167, 08025, Barcelona, Spain. E-mail: jfortea@santpau.cat

From the [1]Sant Pau Memory Unit, Department of Neurology, Hospital de la Santa Creu i Sant Pau, Biomedical Research Institute Sant Pau, Universitat Autònoma de Barcelona, Barcelona, Spain; [2]Center of Biomedical Investigation Network for Neurodegenerative Diseases (CIBERNED), Madrid, Spain; [3]Barcelona Down Medical Center. Fundació Catalana Síndrome de Down, Barcelona, Spain; and [4]Department of Psychology, Centre for Lifespan Changes in Brain and Cognition, University of Oslo, Oslo, Norway

Additional supporting information can be found in the online version of this article.

continuum in sporadic AD.[4,5] There is a strong convergence of findings reporting increases in myo-inositol (mI), a marker of astrocytosis neuroinflammation, and decreases in N-acetylaspartate (tNAA), a neuronal marker, with disease progression in various brain areas.[4–8] This metabolic signature correlates to both in vivo imaging measures of amyloid[5,6,9] and to postmortem AD pathology.[10]

The few MRS studies in people with DS have identified a similar pattern of changes in MRS metabolites, with increases of mI and decreases of tNAA. These changes might arise from AD-related pathological alterations, but in the case of mI, could also result from the presence of the mI transporter gene in the chromosome 21.[11,12] However, the temporality of MRS changes with age and their relationship with core-AD biomarkers and brain atrophy is still unknown.

Taking advantage of the Down Alzheimer Neuroimaging Initiative (DABNI), a large cohort of adults with DS with available magnetic resonance imaging (MRI), MRS, positron emission tomography (PET), and cerebrospinal fluid (CSF) biomarkers, we aimed to determine the metabolite levels changes (1) with age, and (2) along the diagnostic groups of the AD continuum, and assess the relationship between metabolite alterations, and (3) core-AD CSF biomarkers, and (4) cortical thickness.

Methods

Participants

This is a single-center cross-sectional study. We recruited 118 adults with DS aged 18 years or older from the population-based DABNI cohort.[3] We also included a convenience sample of 71 cognitively normal euploid subjects (controls) from the Sant Pau Initiative of Neurodegeneration SPIN cohort.[13] The study was approved by the Sant Pau Research Ethics Committee, following the standards for medical research in humans recommended by the Declaration of Helsinki. All participants or their legally authorized representatives gave written informed consent.

Adults with DS were clinically evaluated to assess their clinical and cognitive status, including the administration of a semi-structured health questionnaire (Cambridge Examination for Mental Disorders of Older People with Down Syndrome [CAMDEX-DS])[14] and a neuropsychological battery including the Cambridge Cognitive Examination for Older Adults with Down's syndrome (CAMCOG-DS) Spanish version.[14] As in previous studies,[3,15] participants were classified during a consensus meeting between the neurologist and neuropsychologist into the following clinical groups: asymptomatic (aDS), when there was no clinical suspicion of AD-related cognitive decline, prodromal AD (pDS), when there was evidence of cognitive decline due to AD, but no significant impact on baseline activities of daily living (ADL), and AD dementia (dDS) when the cognitive decline impacted ADL. This classification was blinded to biomarker data. Eleven individuals were excluded for having medical or psychiatric conditions.

1H-MRS Acquisition and Analysis

MRS was performed on a 3T Philips Achieva magnetic scanner, using the point-resolved spectroscopy single-voxel (PRESS) sequence, with an echo time of 2,000 ms and repetition time of 35 ms, flip angle of 90 degrees, and 1,024 points. The metabolite data profile was acquired in a $2 \times 2 \times 1.1$ mm voxel placed in a region of interest (ROI) located in the posterior cingulate cortex (PCC) and the precuneus. This region was selected due to its reported sensitivity to detect metabolite differences in sporadic AD.[16] We processed MRS data using Spectroscopy Analysis Tools (SPANT) version 1.4.0 (https://martin3141.github.io/spant/index.html), an open-source R toolbox, which relies on iteratively adapted baseline fitting of MRS signal based on multiple penalized splines.[17] We preprocessed the raw MRS data removing the residual water signal using an HSVD filter, and realigning the data to 2.01 reference point (tNAA peak). We then run the SPANT::fit_mrs() with the ABFIT method to quantify different metabolites, providing measures for mI, tNAA, and total Cr (TCr). We used the ratio by TCr (phosphocreatine + creatine) for the two metabolites (ie, ml and tNAA) in all statistical analyses given the stability of its resonance peak.[8] Moreover, TCr did not change along the age-span in our sample (both DS and controls with Spearman rho <0.15, data not shown), as previously shown in the literature.[8] Moreover, by normalizing with TCr, we control interindividual differences that might arise from different amounts of water due to atrophy and/or voxel location. Quality control criteria included a signal-to-noise ratio higher than 5, a FWHM lower than 0.15 ppm, and a Q value (a measure of quality fitting)[18] lower than 2. In addition, SPANT provides estimated SDs (based on Cramér-Rao lower bounds), which reflect the quality of the expected fitting. Due to the disease-associated changes, the SDs in a cohort along the whole AD continuum are increased with respect to those in homogeneous samples. Thus, we imposed a liberal threshold of less than 50% of SDs as a quality criterion. Four participants did not fulfill the aforementioned quality control criteria.

CSF Acquisition and Analysis

A subset of 73 adults with DS underwent a lumbar puncture to obtain CSF sampling, following international recommendations.[19] We measured core AD biomarkers

($A\beta_{42}$, $A\beta_{40}$, and phosphorylated tau 181 -pTau) using the Lumipulse G assays on LUMIPULSE G600II automated platform (Fujirebio). In addition, we quantified CSF levels of YKL-40 (chitinase-3-like protein 1), a marker of reactive astroglia in AD,[20] and neurofilament light (NfL), a marker of neurodegeneration,[21,22] using ELISA Kit MicroVue (Quidel, San Diego, CA, USSA) and NF-light (UmanDiagnostics, Umeå, Sweden), respectively. All euploid controls had normal core AD biomarkers levels, assessed in the same conditions and with the same technique.[13]

Amyloid PET Acquisition and Processing

A subset of 38 participants with DS also underwent an amyloid PET scan using the tracer 18F-florbetapir. We initially only offered amyloid PET to those subjects that also consented to CSF analyses due to grant protocol restraints. We had to stop the florbetapir PET recruitment due to restricted access in Spain for research. Florbetapir PET was acquired using a Philips Gemini TF scan 50 minutes after injection of 370 mBq of 18F-florbetapir, with 2 mm slice thickness and 128 × 128 image size. The images were processed to obtain a unique value that represents the global amyloid load in the brain.[23] Briefly, florbetapir PET images were normalized to a standard space using a two-step registration approach: native florbetapir image to structural T1-weighted MRI, and T1-weighted MRI to standard MNI152 template. We computed a global amyloid PET measure, averaging the signal across the cingulate, parietal, frontal, and temporal cortical areas, previously normalized using the whole cerebellum as the reference regions. Such global amyloid scalar value, referenced as Landau's florbetapir signature throughout the manuscript, has been shown to accurately differentiate amyloid positive patients in sporadic AD.

Structural T1-MRI Acquisition and Processing

Structural T1-weighted images were acquired with a 3 Tesla Philips Achieva scanner, using an MPRAGE protocol with 0.94 × 0.94 × 1 mm voxel resolution, 8.1 ms and 3.7 ms of repetition time and echo time, respectively, and 160 slices. We computed cortical thickness using the Freesurfer package version 6.0 (https://surfer.nmr.mgh.harvard.edu/) following a procedure previously described.[24,25] Briefly, Freesurfer automatically delineates the white matter and pial surfaces in order to compute a cortical thickness value for each vertex in the brain. Each individual cortical thickness map is then normalized to the standard space (*fsaverage*) and smoothed using a gaussian kernel of 15 mm. From the initial set of 108 adults with DS with good quality MRS data, 26 subjects were excluded due to erroneous segmentation.

Statistical Analysis

The age-associated trajectory of each metabolite was assessed with a within-group linear regression model, as implemented in the R package.

To assess differences in baseline demographic characteristics and metabolites levels between the diagnostic groups, we used a Kruskal–Wallis rank sum test, with pairwise comparisons using the Dwass–Steel–Critchlow–Fligner test. In addition, for the metabolite analyses, we controlled for multiple comparisons using the Benjamin and Hochberg false discovery rate (FDR) method. All these analyses were performed using the R package *StatsExpressions*.[26]

To test the diagnostic performance of each metabolite, we used receiver operating characteristic (ROC) curves and assessed the area under the curve (AUC) for each metabolite. We used the Youden's index to compute the optimal threshold that differentiates between the clinical groups.

To investigate the relationship between the metabolite's ratio levels and AD biomarkers (ie, ratio $A\beta_{42}/A\beta_{40}$, pTau, YKL-40, NfL, and Landau's florbetapir signature), we performed Spearman correlation tests both in all adults with DS and separately in aDS and symptomatic DS (ie, pooling pDS and dDS together due to the relatively small sample size). We considered significant those correlations with a p value < 0.05 after controlling for multiple comparisons using the Benjamin and Hochberg FDR test. To further visualize the stability of our associations, we ran bootstrap analyses, subsetting and shuffling our DS sample 1,000 times using the R package *boot* and recomputing the Spearman Rho estimate using the package *ppcor*. We plotted the original estimate and the interquartile range of these 1,000 permutations.

Finally, to study the association between metabolite ratios and cortical thickness, we used a general linear model with sex as a nuisance factor, for each vertex of the surface, as implemented in Freesurfer. We performed this analysis for the whole DS sample, and aDS and symptomatic patients separately. We controlled for false positive results using a cluster-extent Monte Carlo approach, also implemented in Freesurfer.[27] Only results that survived multiple comparisons (FWE $p < 0.05$) are shown. Adjusting by age in autosomal dominant AD and DS studies is a topic of debate, addressed with different approaches in the literature. In DS, AD pathology is universal by age 40 years, and the cumulative incidence is over 90% in the seventh decade. Therefore, the concept of healthy aging in this population is very problematic and very difficult to dissect from preclinical AD (ie, we cannot remove the effect of normal aging from that of the disease process). However, on the other hand, the shared

association with age of several variables makes the epiphenomenological association between such variables problematic. Hence, in the present study, we decided to perform both adjusted and unadjusted (by age) statistical analyses. For the group comparisons, in addition to the nonparametric approach, we repeated the analyses using an analysis of covariance (ANCOVA). We also performed the ROC analyses adjusting by age. For the association between AD-core biomarkers, we corrected age-related effect using a partial Spearman correlation. For cortical thickness analyses, we re-ran the analyses using a GLM with age as a nuisance factor, as implemented in Freesurfer.

Results

Sample

The final sample included 71 controls and 103 adults with DS, of whom 62 were asymptomatic, 21 pAD, and 20 dAD. The Table shows the demographics and biomarker data of the participants. As expected, there were significant statistical differences in age and all biomarker levels between the different clinical groups.

Changes in MRS Metabolites Profiles along the AD Continuum in DS

Figure 1A shows the relationship between age and both mI/TCr and tNAA/TCr in adults with DS and controls. The mI/TCr was increased in all DS compared with controls, and further increased in the early 40s. The tNAA/TCr decreased with age in both adults with DS and controls. Asymptomatic adults with DS showed comparable tNAA levels as controls, although tNAA levels started to decrease in their mid-40s.

Figure 1B shows the mI/TCr and tNAA/TCr ratios along the AD continuum. There were significant group differences for both mI/TCr ($p < 0.001$) and tNAA/TCr ($p = 0.002$). All the DS subgroups had a higher mI/TC ratio than controls ($p < 0.001$ FDR corrected). The pDS and dDS groups had increased levels compared to aDS (both with $p < 0.01$ after FDR corrected), but there were no significant differences between pDS and dDS. We

TABLE. Participants Demographics

	Controls (N = 71)	All Down syndrome (N = 103)	Asymptomatic Down syndrome (N = 62)	Prodromal Down syndrome (N = 21)	Demented Down syndrome (N = 20)	Statistical Differences (*p* value)
Age	54.3 (49.4–57.1)	44.8 (36.9–53.2)	40.2 (31–46.3)	49.8 (44.8–53.6)	54.1 (49.9–56.2)	<0.001
Sex (N female)	45	39	25	7	7	0.118
Total CAMCOG	NA	74 (58–83)	78 (65–85)	73 (58–78)	52 (39–63)	<0.001
CSF $A\beta_{42}/A\beta_{40}$ ratio	NA	0.061 (0.042–0.084)	0.08 (0.062–0.094) (N = 35)	0.041 (0.030–0.051) (N = 31)		<0.001
Florbetapir Landau Signature (SUVr)	NA	1.16 (1.02–1.3)	1.04 (1–1.19) (N = 24)	1.27 (1.21–1.37) (N = 14)		0.002
CSF pTau 181 (pg/ml)	NA	58.7 (27.9–122.7)	29.6 (17.1–56.7) (N = 40)	146.4 (96.3–209.6) (N = 33)		<0.001
CSF NfL (pg/ml)	NA	475.5 (305.4–764.5)	353.2 (201–450.1) (N = 36)	766.3 (684.5–1618.5) (N = 28)		<0.001
CSF YKL-40 (ng/ml)	NA	107.3 (90.4–214.2)	134 (70–178) (N = 34)	206.3 (204.6–323) (N = 18)		<0.001

Table shows median value and inter quartiles from the median.
CAMCOG = Cambridge Cognitive Examination for Older Adults with Down's syndrome; CSF = cerebrospinal fluid; NA = not applicable NfL = neurofilament light.

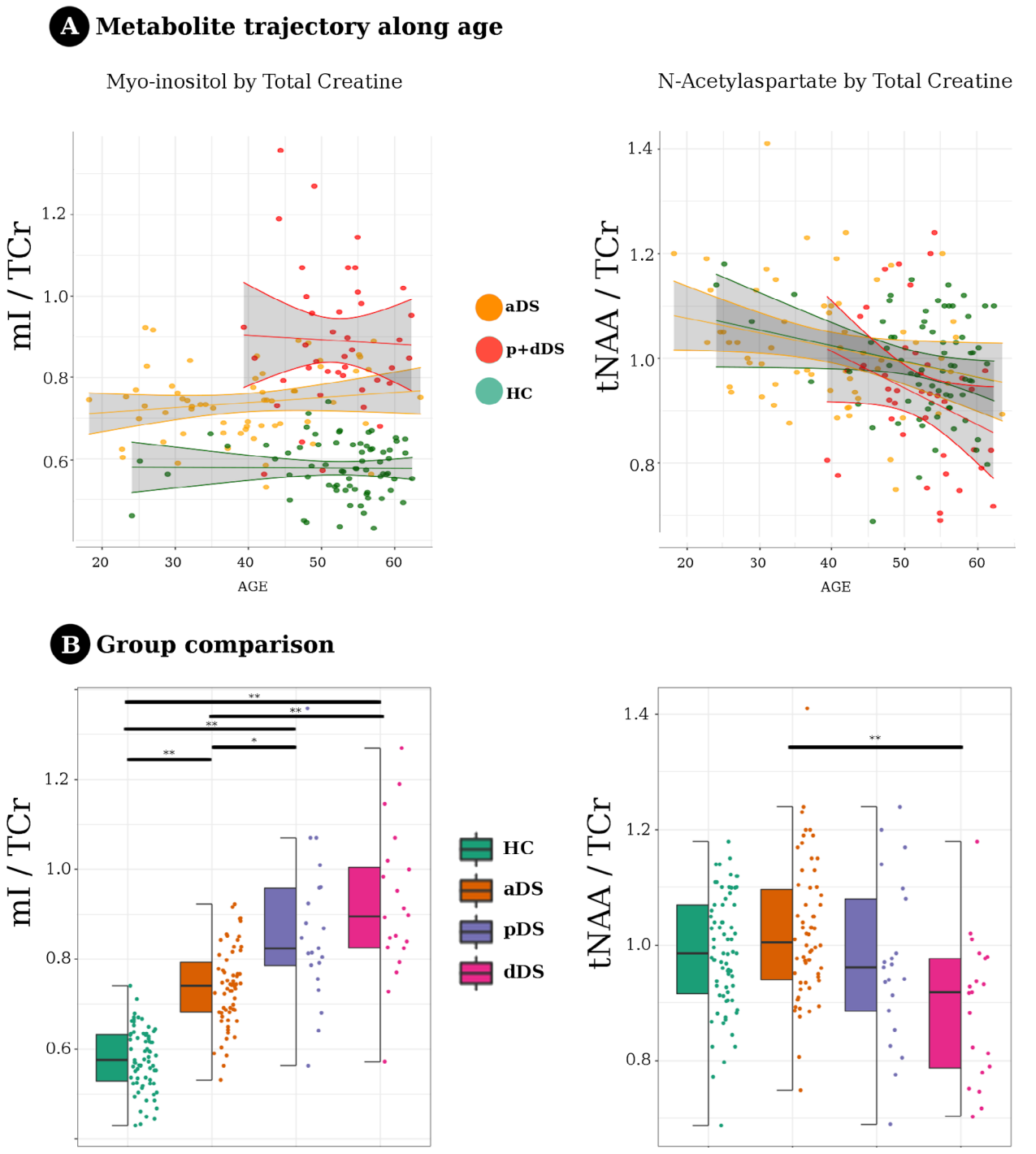

Color Figure - Print and Online

FIGURE 1: The myo-inositol (mI) and N-acetylaspartate (tNAA) changes with age and along the Alzheimer's disease (AD) continuum in Down syndrome. (A) The association for mI/total creatine (TCr) (left) and tNAA/TCr (right) with age. Lines were obtained fitting a linear model for each subgroup. (B) Boxplot (median and interquartile ranges) and data-point distribution for mI/TCr (left) and tNAA/TCr (right) for each subgroup. aDS = asymptomatic Down Syndrome; dDS = Down Syndrome with dementia; HC = euploid healthy controls; pDS = prodomal Down Syndrome; ** = $p < 0.01$ FDR corrected; * = $p < 0.05$ false discovery rate (FDR) corrected.

identified the same pattern of significant results when adjusting the comparisons by age. The ROC analyses showed an AUC of 0.74 (cutoff point = 0.786; confidence interval [CI] = 0.76–0.87) and 0.85 (cutoff point = 0.824; CI = 0.77–0.89), when comparing aDS versus pDS and aDS versus dDS, respectively. For the tNAA/TCr ratio, the pairwise comparisons only revealed statistical differences between aDS and dDS (p = 0.001

FDR corrected). In the ROC analyses, the AUC analyses showed an AUC of 0.62 (cutoff point = 0.98; CI = 0.88–1.00) and 0.78 (cutoff point = 0.938; CI = 0.89–1.03), when comparing aDS versus pDS and aDS versus dDS, respectively. We found similar results when adjusting by age. Concretely, for mI, we obtained an AUC of 0.75 and 0.88 when comparing aDS against pDS and dDS, respectively, and an AUC of 0.65 and 0.82 when comparing tNAA levels of aDS against pDS and dDS, respectively.

Metabolite Associations with Core AD and Inflammatory Biomarkers

We next studied the relationship between both the mI/TC and tNAA/TC ratios and AD biomarkers (Fig 2). The mI/TC ratio was significantly associated with amyloid biomarkers, both with the CSF $A\beta_{42}/A\beta_{40}$ ratio and with the Landau's florbetapir signature in the whole sample of DS ($p < 0.05$ FDR corrected for both biomarker). However, when splitting our sample into subgroups, only those with symptomatic AD showed a significant association with CSF $A\beta_{42}/A\beta_{40}$ ratio. The mI/TC ratio was also significantly associated with CSF pTau levels in the whole sample ($p < 0.05$ FDR corrected). When splitting the sample, no association survived multiple comparisons. We also found a significant positive association between the mI/TCr ratio and CSF NfL both in the whole sample and in the symptomatic AD subgroup ($p < 0.05$ FDR corrected). We did not find any correlation that survived multiple comparisons between mI/Tcr and CSF YKL-40. The tNAA/TCr ratio was associated with Laundau's florbetapir signature in both the whole sample and in aDS (both $p < 0.05$, uncorrected), but these associations did not survive multiple comparisons. The tNAA/TCr ratio was also associated with CSF NfL in the whole sample and in the symptomatic AD subgroup (both $p < 0.05$, uncorrected). When adjusting correlations by age using partial Spearman correlation, we found similar results.

Cortical Thickness is Associated with MRS Metabolite Alterations

Figure 3 shows the association between the mI/TCr and tNAA/TCr ratios and cortical thickness in the whole sample and in symptomatic patients. We found a widespread pattern of cortical thinning with increasing mI/TC ratios in AD vulnerable regions, encompassing the precuneus,

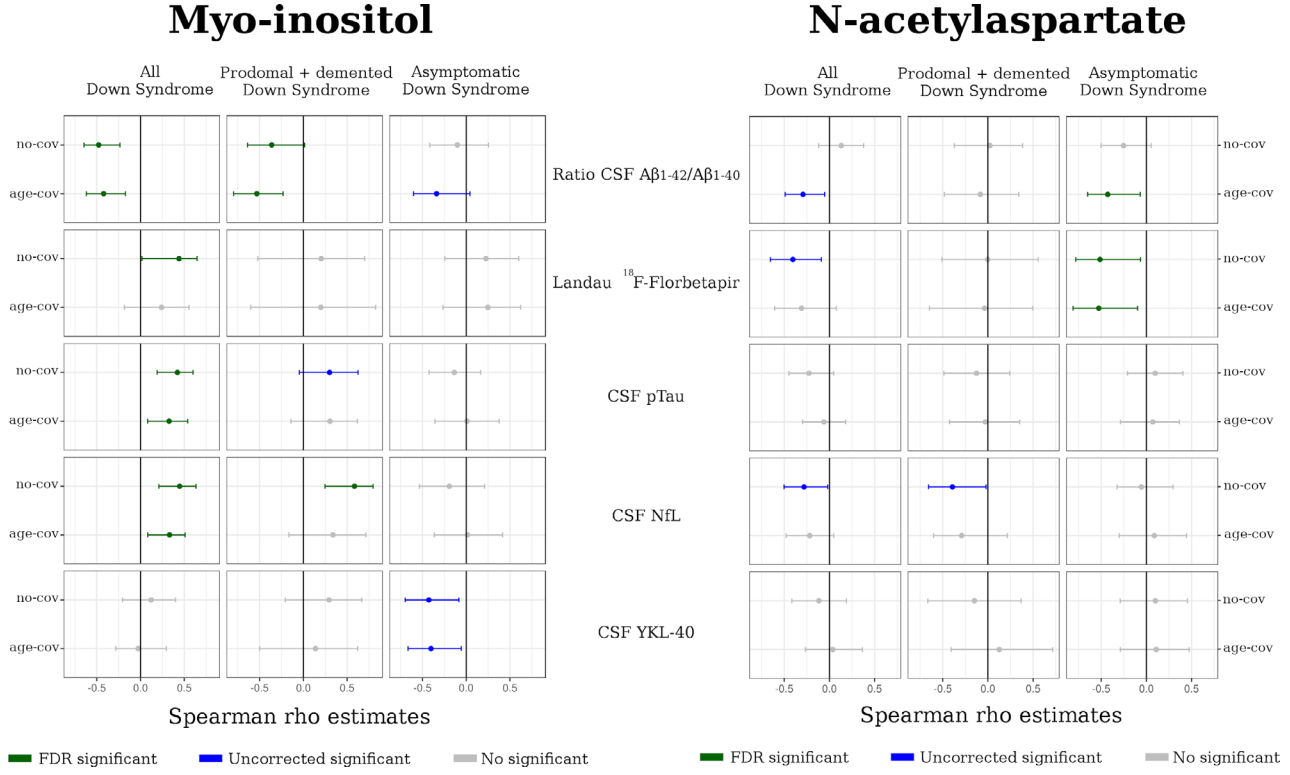

FIGURE 2: The myo-inositol (mI) and N-acetylaspartate (tNAA) correlate with Alzheimer's disease (AD)-core biomarkers. Association between AD biomarkers and mI/total creatine TCr and tNAA/TCr for the whole sample (left column), prodromal and Down Syndrome with dementia (central column), and asymptomatic Down Syndrome (right column). Midpoint shows the (partial) Spearman Rho value for the included sample, whereas the line represents the confidence interval (CI) for bootstrap with 1,000 permutations. For each biomarker, we compute both the adjusted (age-cov) and no-adjusted (no-cov) Spearman Rho value. CSF = cerebrospinal fluid; FDR = false discovery rate.

Color Figure - Print and Online

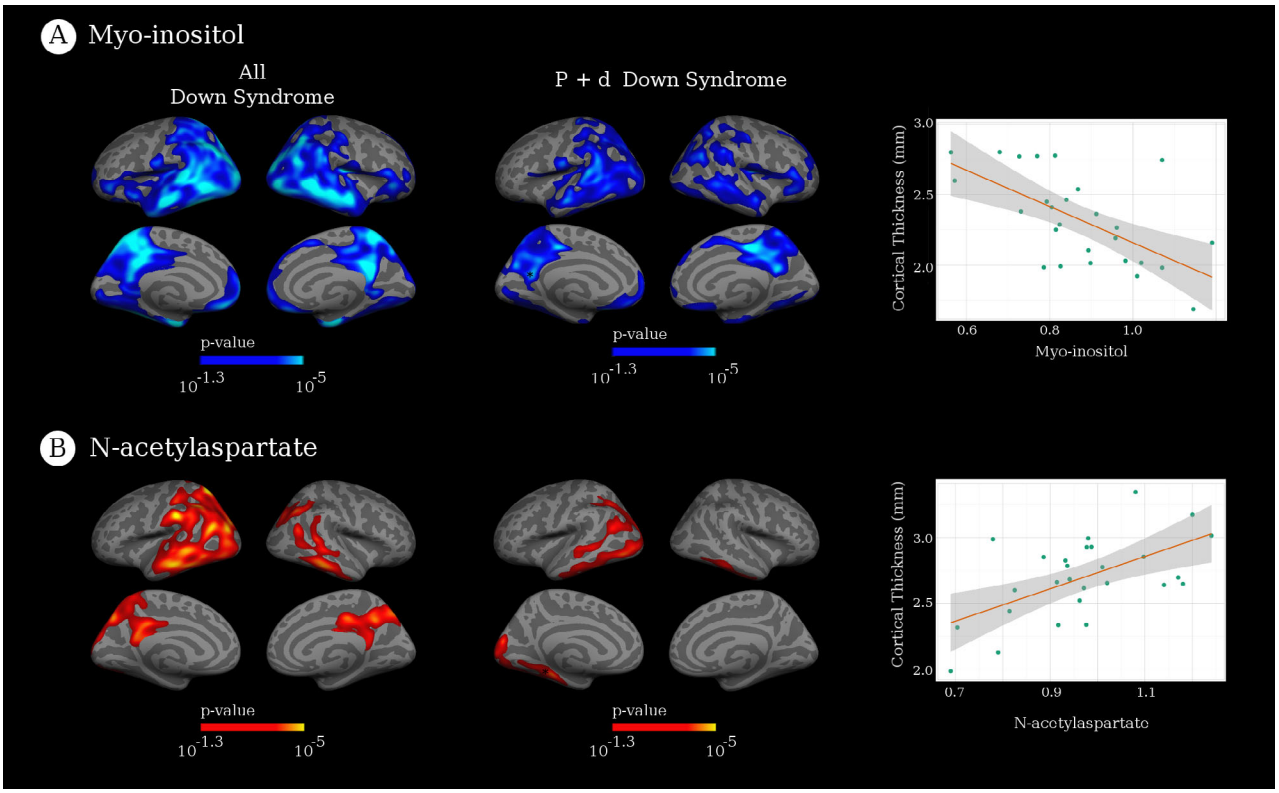

Color Figure - Print and Online

FIGURE 3: The myo-inositol (mI) and N-acetylaspartate (tNAA) are related to cortical atrophy in the Alzheimer's disease (AD) continuum in Down syndrome. Cortical surface representation of significant negative (blue) association between mI/total creatine (TCr) and cortical thickness and positive (red) association between tNAA/TCr. Scatterplots show the associations for the most significant vertex (marked with black *).

temporo-parietal, and lateral temporal areas bilaterally, the medial temporal in the right hemisphere, and part of the medial inferior frontal cortex in the left hemisphere. This association was mainly driven by symptomatic patients. Similarly, the tNAA/TCr ratio was associated with cortical thickness in an overlapping (but less extended) pattern, both in the whole sample and in symptomatic patients. We found no significant association between the mI/TC ratio and cortical thickness in the aDS subgroup, and only a small cluster in the left superior frontal gyrus for the tNAA/TCr analysis (results not shown). When adjusting by age, we found a similar pattern of results, even though no cluster-extend multiple comparisons clusters survived for the tNAA analyses.

Discussion

This study investigated for the first time the MRS changes with age and along the AD continuum, as well as their diagnostic performance and association with core AD, inflammatory biomarkers, and cortical thickness. Metabolite levels are altered in symptomatic AD and are associated with core AD biomarkers changes in adults with DS. Despite the lower diagnostic performance with respect core AD biomarkers, MRS is able to track AD-related neuroinflammatory and neurodegenerative changes, and has the advantage with respect CSF or PET biomarkers, that it could be easily included in the MRI acquisition in longitudinal studies. MRS could thus be used as a disease-staging biomarker in DS, with potential of demonstrating target engagement in disease-modifying therapies.

This study showed MRS metabolic alterations associated with DS and with AD pathophysiology. The mI/TCr had clear differences even in the youngest asymptomatic individuals (and throughout all ages) with respect to controls, whereas the tNAA/TCr was unchanged in asymptomatic individuals. These results underscore the importance of considering the neurodevelopmental or constitutive differences in individuals with DS when interpreting biomarker results.[3] The increases of mI in asymptomatic DS individuals are not only a result of aging, as previously reported for the general population,[28–30] but probably also due to the presence of the inositol transporter gene on chromosome 21[12] and/or a consequence of neuroinflammation[31–33] resulting from an increase in inflammatory cytokine expression.[34] A prior study with a smaller sample size[11] (17 aDS and 5 dDS) also found

increases in mI in aDS compared with controls, but was not able to detect differences between the DS subgroups. We did find changes both in the mI/TC and tNAA/TC ratios along the AD continuum. The larger sample size in our study enabled us the identification of a gradient of increases along the AD continuum in the mI/TC ratio. These results are congruent with previous reports in sporadic AD, in which participants with mild cognitive impairment and AD dementia showed increases in the mI/TC ratio compared to controls.[4,5,7,8,35,36] The tNAA/TC ratio was less sensitive to detect changes with disease progression. We only found differences in the aDS versus dDS comparison, in agreement with previous reports.[11] Further research positioning the MRS voxel in a more prominent and early-stage neurodegeneration region, such as the temporal cortex, might enhance the sensitivity of tNAA/TCr. Despite the differences between clinical groups, the ROC analyses for MRS showed lower diagnostic performance than plasma or CSF biomarkers.[3]

This study also assessed the relationship between MRS metabolite alterations and AD biomarkers. The mI/TC ratio was more strongly associated with AD biomarkers than tNAA, and was the only metabolite to survive multiple comparisons correction. The mI/TC ratio was associated with amyloid biomarkers (both the CSF $A\beta_{42}/A\beta_{40}$ ratio and amyloid PET uptake), CSF pTau, and CSF NfL levels in the whole sample, and with the CSF $A\beta_{42}/A\beta_{40}$ ratio and CSF NfL (and a trend for CSF pTau levels) in the symptomatic patients. Previous studies had also found a positive association between mI and amyloid PET uptake[5,6,9] or amyloid neuropathology[10] in sporadic AD. In our study, mI was also correlated with tau and neurodegeneration markers. Although previous studies in sporadic AD did not find an association between neurofibrillary tangles and mI,[10] others have shown a colocalization of neurofibrillary tangles and reactive astrocytes (see Laurent et al[37] for a review), suggesting a possible association between both markers. Alternatively, the positive correlation between mI and CSF pTau might be driven by the group differences along the AD continuum as the association within each subgroup did not survive the multiple comparison correction in the stratified analyses. Further studies using in vivo local measures of tau pathological changes (such as tau PET) might resolve these discrepancies between CSF biomarkers and postmortem quantifications.

Contrary to our expectations, there were no associations between mI and CSF YKL-40 levels (only a counterintuitive negative association in asymptomatic subjects). This is surprising given that both mI and YKL-40 have been proposed as markers of astrocytosis,[20] and both are increased with disease progression.[4,38] It is possible that both biomarkers reflect different astrocytic and neuroinflammatory responses in AD, or that they track changes in different astrocyte subtypes.[39,40] This suggests to us that the inflammatory processes measured by both biomarkers are different. The inflammatory response in AD is complex and probably evolves in different phases along the disease course. Further research using in vivo markers of inflammation (such as deprenyl or SMBT-1 PET tracer) or animal studies will help further understand these associations. Although no correlation survived multiple comparisons correction for tNAA, we found significant (uncorrected) correlations between tNAA and both CSF NFL levels and florbetapir PET uptake. As expected, the correlation with amyloid biomarkers were found in asymptomatic subjects, and the correlation with neurodegeneration in symptomatic subjects.

Metabolite levels are also associated with neurodegeneration. We found an association between both the mI/TC and tNAA/TC ratios in the precuneus and the cortical thinning in widespread regions typically affected in AD. Of note, the AD-vulnerable regions are similar in sporadic amnesic AD[25,41] and DS.[3,42,43] These associations were more prominent in symptomatic stages of the disease. To our knowledge, it is the first study reporting these relationships in DS. In sporadic AD, there are some previous reports assessing the association between MRS metabolites and local neuroimaging changes in AD. For instance, a recent work by Sheikh-Bahaei and colleagues[9] investigated the local relationship between metabolite levels and amyloid and FDG PET uptake. Others have focused on the local relationship between structural imaging alterations and metabolites levels in subcortical regions and the white matter, using both whole-brain MRS,[44,45] or investigating specific structures, such as the hippocampus.[46] However, no previous study had assessed the impact of the metabolite signature on the whole cortical mantle.

The main strength of this study is the inclusion of a large population-based cohort of adults with DS with available multimodal biomarker data, including MRS, MRI, florbetapir PET, and CSF biochemical biomarkers. The population-based cohort of adults with DS with subjects in all the clinical stages of the AD continuum and the control group helped to disentangle the neurodevelopmental and AD-associated changes. Furthermore, the multimodal assessments helped us to investigate the relationship with the AD pathophysiology. Despite the lower diagnostic performance of MRS with respect to plasma or CSF biomarkers, our results suggest that MRS can detect neuroinflammatory and neurodegenerative changes associated with AD in adults with DS. MRS is more accessible (and far cheaper) than PET studies and

easier to implement in longitudinal designs than CSF studies. Therefore, MRS could be used to assess target engagement or as surrogate markers of efficacy in disease modifying therapies.

This study also has limitations. Metabolite levels were assessed in only one specific location using single-voxel MRS. The acquisition of multi-voxel MRS could provide further insights into the pattern of metabolite alterations beyond the precuneus. Moreover, our MRS acquisition protocol is not suitable to use state-of-the-art models, such as the MRS-diffusion model, that would allow the measurement not only of metabolite levels, but also the measurement of the within-cellular displacement of metabolites that might change due to glia morphological alterations in early stages of the disease.[47] In addition, the discrepancies between mI and CSF YKL-40 suggest that further work, with more specific cytokine-expression should be done to understand the origin of the mI alterations. Finally, longitudinal studies are required to better characterize the longitudinal alterations of these metabolites in a single-subject basis.

In summary, this study supports the use of MRS to characterize pathophysiological alterations in DS and its potential to track AD pathophysiology in AD clinical trials in DS.

Acknowledgments

This study was supported by the Fondo de Investigaciones Sanitario, Instituto de Salud Carlos III, and the CIBERNED programme, partly jointly funded by the EU European Regional Development Fund. This work was also supported by the National Institutes of Health, Departament de Salut de la Generalitat de Catalunya, Pla Estratègic de Recerca i Innovacio en Salut, and Fundació La Marató de TV3. V.M. is supported by the Fondo de Investigaciones Sanitario, Instituto de Salud Carlos III. M.F.I. is supported by the Jérôme Lejeune and Sisley D'Ornano Foundations. A.B. is supported from a Juan de la Cierva-Incorporacion grant from the Spanish Ministery of Economy (IJCI-2017-32609) and a Miguel Servet I grant (2020, CP20/00038) from the Carlos III Health Institute. Fundació Catalana Síndrome de Down, Fundació Víctor Grífols i Lucas, and the Jérôme Lejeune Foundation also partly supported this work. Finally, this work was supported by Generalitat de Catalunya and a grant from the Fundació Bancaria La Caixa to R.B. We thank all the participants with Down's syndrome, their families, and their carers for their support of, and dedication to, this research. We also acknowledge the Fundació Catalana Síndrome de Down for global support; Laia Muñoz, Soraya Torres, and Shaimaa El Bounasri for laboratory and sample handling; Reyes Alcoverro, Marta Salinas, and Tania Martínez for administrative support; and Concepción Escola and Diana Garzón for nursing handling.

Author Contributions

V.M., I.B., A.L., and J.F. contributed to the conception and design of the study. A.B., J.P., M.A., D.V.P., D.A., R.B., M.C.I., M.A., B.B., L.V., S.F., C.P., and F.I. contributed to the acquisition and analysis of data. V.M. and J.F. contributed to drafting the text and preparing the figures. Names and institutional affiliations and contributions of the Down Alzheimer Barcelona Neuroimaging Initiative study group members are included in a Supplementary Table.

Potential Conflicts of Interest

Authors declared no potential conflicts of interest.

References

1. Rubenstein E, Hartley SL, Bishop L. Epidemiology of dementia and Alzheimer disease in individuals with Down syndrome. JAMA Neurol 2019;77:262–264.
2. Dubois B, Feldman HH, Jacova C, et al. Advancing research diagnostic criteria for Alzheimer's disease: the IWG-2 criteria. Lancet Neurol 2014;13:614–629.
3. Fortea J, Vilaplana E, Carmona-Iragui M, et al. Clinical and biomarker changes of Alzheimer's disease in adults with Down syndrome: a cross-sectional study. Lancet 2020;395:1988–1997.
4. Kantarci K, Jack CR, Xu YC, et al. Regional metabolic patterns in mild cognitive impairment and Alzheimer's disease: a 1H MRS study. Neurology 2000;55:210–217.
5. Voevodskaya O, Sundgren PC. Myo-inositol changes precede amyloid pathology and relate to APOE genotype in Alzheimer disease. Neurology 2016;86:1754–1761.
6. Kantarci K, Lowe V, Przybelski SA, et al. Magnetic resonance spectroscopy, beta-amyloid load, and cognition in a population-based sample of cognitively normal older adults. Neurology 2011;77:951–958.
7. Voevodskaya O, Poulakis K, Sundgren P, et al. Brain myoinositol as a potential marker of amyloid-related pathology: a longitudinal study. Neurology 2019;92:e395–e405.
8. Valenzuela MJ, Sachdev PS. Magnetic resonance spectroscopy in AD. Neurology 2011;56:592–598.
9. Sheikh-bahaei N, Manavaki R, Sheikh-bahaei N. PET-guided MR spectroscopy in Alzheimer's disease. Ann. Neurol (in press).
10. Murray ME, Przybelski SA, Lesnick TG, et al. Early Alzheimer's disease neuropathology detected by proton MR spectroscopy. J Neurosci 2014;34:16247–16255.
11. Lin A-L, Powell D, Caban-Holt A, et al. ^{1}H-MRS metabolites in adults with Down syndrome: effects of dementia. NeuroImage Clin 2016;11:728–735.
12. Berry GT, Mallee JJ, Kwon HM, et al. The human osmoregulatory Na+/myo-inositol cotransporter gene (SLC5A3): molecular cloning and localization to chromosome 21. Genomics 1995;25:507–513.
13. Alcolea D, Clarimón J, Carmona-Iragui M, et al. The Sant Pau Initiative on Neurodegeneration (SPIN) cohort: a dataset for biomarker

discovery and validation in neurodegenerative disorders. Alzheimers Dement (N Y) 2019;5:597–609.

14. Esteba-Castillo S, Dalmau-Bueno A, Vidal N, et al. Adaptación y validación del Cambridge examination for mental disorders of older people with Down's syndrome and others with intellectual disabilities (CAMDEX-DS) en población española con discapacidad intelectual. Rev Neurol 2013;57:337.
15. Fortea J, Carmona-Iragui M, Benejam B, et al. Plasma and CSF biomarkers for the diagnosis of Alzheimer's disease in adults with Down syndrome: a cross-sectional study. Lancet Neurol 2018;17:860–869.
16. Öz G, Alger JR, Barker PB, et al. Clinical proton MR spectroscopy in central nervous system disorders. Radiology 2014;270:658–679.
17. Wilson M. Adaptive baseline fitting for ^{1}H MR spectroscopy analysis. Magn Reson Med 2021;85:13–29.
18. Wilson M, Reynolds G, Kauppinen R, et al. A constrained least-squares approach to the automated quantitation of in vivo ^{1}H magnetic resonance spectroscopy data. Magn Reson Med 2011;65:1–12.
19. Vanderstichele HMJ, Janelidze S, Demeyer L, et al. Optimized standard operating procedures for the analysis of cerebrospinal fluid Aβ42 and the ratios of Aβ isoforms using low protein binding tubes. J Alzheimers Dis 2016;53:1121–1132.
20. Querol-Vilaseca M, Colom-Cadena M, Pegueroles J, et al. YKL-40 (Chitinase 3-like I) is expressed in a subset of astrocytes in Alzheimer's disease and other tauopathies. J Neuroinflammation 2017;14:1–10.
21. Gaetani L, Blennow K, Calabresi P, et al. Neurofilament light chain as a biomarker in neurological disorders. J Neurol Neurosurg Psychiatry 2019;90:870–881.
22. Delaby C, Alcolea D, Carmona-Iragui M, et al. Differential levels of neurofilament light protein in cerebrospinal fluid in patients with a wide range of neurodegenerative disorders. Sci Rep 2020;10:1–8.
23. Landau SM, Breault C, Joshi AD, et al. Amyloid-β imaging with Pittsburgh compound B and florbetapir: comparing radiotracers and quantification methods. J Nucl Med 2013;54:70–77.
24. Fischl B, Dale AM. Measuring the thickness of the human cerebral cortex from magnetic resonance images. Proc Natl Acad Sci U S A 2000;97:11050–11055.
25. Montal V, Vilaplana E, Alcolea D, et al. Cortical microstructural changes along the Alzheimer's disease continuum. Alzheimer's Dement 2018;14:340–351.
26. Patil I. statsExpressions: "ggplot2" Expressions with Statistical Details. 2019.
27. Hagler DJ, Saygin AP, Sereno MI. Smoothing and cluster thresholding for cortical surface-based group analysis of fMRI data. Neuroimage 2006;33:1093–1103.
28. Reyngoudt H, Claeys T, Vlerick L, et al. Age-related differences in metabolites in the posterior cingulate cortex and hippocampus of normal ageing brain: a 1H-MRS study. Eur J Radiol 2012;81:e223–e231.
29. Suri S, Emir U, Stagg CJ, et al. Effect of age and the APOE gene on metabolite concentrations in the posterior cingulate cortex. Neuroimage 2017;152:509–516.
30. Marjańska M, McCarten JR, Hodges J, et al. Region-specific aging of the human brain as evidenced by neurochemical profiles measured noninvasively in the posterior cingulate cortex and the occipital lobe using 1H magnetic resonance spectroscopy at 7 T. Neuroscience 2017;354:168–177.
31. Huggard D, Kelly L, Ryan E, et al. Increased systemic inflammation in children with Down syndrome. Cytokine 2020;127:154938.
32. Wilcock DM, Griffin WST. Down's syndrome, neuroinflammation, and Alzheimer neuropathogenesis. J Neuroinflammation 2013;10:1–10.
33. Patkee PA, Baburamani AA, Long KR, Dimitrova R. Neurometabolite mapping highlights elevated myo-inositol profiles within the developing brain in Down syndrome. Neurobiol Dis 2021;153:105316.
34. Flores-Aguilar L, Iulita MF, Kovecses O, et al. Evolution of neuroinflammation across the lifespan of individuals with Down syndrome. Brain 2020;143:3653–3671.
35. Kantarci K, Xu YC, Shiung MM, et al. Comparative diagnostic utility of different MR modalities in mild cognitive impairment and Alzheimer's disease. Dement Geriatr Cogn Disord 2002;14:198–207.
36. Kantarci K. Proton MRS in mild cognitive impairment. J Magn Reson Imaging 2013;37:770–777.
37. Laurent C, Buée L, Blum D. Tau and neuroinflammation: what impact for Alzheimer's disease and tauopathies? Biom J 2018;41:21–33.
38. Alcolea D, Martínez-Lage P, Sánchez-Juan P, et al. Amyloid precursor protein metabolism and inflammation markers in preclinical Alzheimer disease. Neurology 2015;85:626–633.
39. Liddelow SA, Guttenplan KA, Clarke LE, et al. Neurotoxic reactive astrocytes are induced by activated microglia. Nature 2017;541:481–487.
40. Habib N, McCabe C, Medina S, et al. Disease-associated astrocytes in Alzheimer's disease and aging. Nat Neurosci 2020;23:701–706.
41. Dickerson BC, Bakkour A, Salat DH, et al. The cortical signature of Alzheimer's disease: regionally specific cortical thinning relates to symptom severity in very mild to mild AD dementia and is detectable in asymptomatic amyloid-positive individuals. Cereb Cortex 2009;19:497–510.
42. Matthews DC, Lukic AS, Andrews RD, et al. Dissociation of Down syndrome and Alzheimer's disease effects with imaging. Alzheimers Dement (N Y) 2016;2:69–81.
43. Rafii MS, Lukic AS, Andrews RD, et al. PET imaging of tau pathology and relationship to amyloid, longitudinal MRI, and cognitive change in down syndrome: results from the down syndrome biomarker initiative (DSBI). J Alzheimers Dis 2017;60:439–450.
44. Su L, Blamire AM, Watson R, et al. Whole-brain patterns of 1H-magnetic resonance spectroscopy imaging in Alzheimer's disease and dementia with Lewy bodies. Transl Psychiatry 2016;6:1–8.
45. Constans JM, Meyerhoff DJ, Gerson J, et al. H-1 MR spectroscopic imaging of white matter signal hyperintensities: Alzheimer disease and ischemic vascular dementia. Radiology 1995;197:517–523.
46. Kantarci K, Petersen RC, Przybelski SA, et al. Hippocampal volumes, proton magnetic resonance spectroscopy metabolites, and cerebrovascular disease in mild cognitive impairment subtypes. Arch Neurol 2008;65:1621–1628.
47. Ligneul C, Palombo M, Hernández-Garzón E, et al. Diffusion-weighted magnetic resonance spectroscopy enables cell-specific monitoring of astrocyte reactivity in vivo. Neuroimage 2019;191:457–469.